PERGAMON
www.elsevier.com/locate/watres

Wat. Res. Vol. 34, No. 2, pp. 528–538, 2000

Printed in Great Britain
PII: S0043-1354(99)00147-5
0043-1354/99/$ - see front matter

COMBINED EFFECT OF SUBSTRATE CONCENTRATION AND FLOW VELOCITY ON EFFECTIVE DIFFUSIVITY IN BIOFILMS

HALUK BEYENAL and ZBIGNIEW LEWANDOWSKI*[M]
Center for Biofilm Engineering, PO Box 173980, Room 366 EPS, Montana State University, Bozeman, MT 59717-3980, USA

(First received 1 November 1998; accepted in revised form 1 March 1999)

Abstract—We have evaluated the influence of glucose concentration and flow velocity at which biofilms were grown on the distribution of effective diffusivity in biofilms consisting of *Pseudomonas aeruginosa, Pseudomonas fluorescens*, and *Klebsiella pneumoniae*. From the local diffusivity profiles, measured by a novel microelectrode, the surface averaged relative effective diffusivities (D_s) were calculated at different depths in the biofilms. The D_s decreased toward the bottom of the biofilms and the D_s profiles were affected by growth conditions. The D_s was higher in biofilms grown at high glucose concentrations and at low flow velocities; and it was influenced by the glucose concentration to a much larger extent than by the flow velocity. © 1999 Elsevier Science Ltd. All rights reserved

Key words—biofilms, effective diffusivity, biofilm modeling, biofilm structure

NOMENCLATURE

A	sensing area of microelectrode (m^2)
A_d	surface area available for diffusion in diffusion cell (m^2)
b	number of mole of electrons transferred in the reaction
C_g	glucose concentration (kg/m^3)
C_o	bulk ferricyanide concentration (mol/m^3)
C_s	ferricyanide concentration at the tip of the microelectrode (mol/m^3)
D	molecular diffusivity of ferricyanide in the electrolyte solution (m^2/s)
D_{ag}	effective diffusivity of ferricyanide in the agar gel layer (m^2/s)
D_a	average relative effective diffusivity of ferricyanide in the biofilm
D_{CN}	diffusivity of ferricyanide (m^2/s)
D_l	local relative effective diffusivity of ferricyanide in the biofilm
D_s	surface averaged relative effective diffusivity of ferricyanide in the biofilm
D_i	effective diffusivity of ferricyanide in the medium i (m^2/s)
D_m	effective diffusivity of ferricyanide in the membrane (m^2/s)
D_{ma}	effective diffusivity of ferricyanide in the membrane and the agar gel layers (m^2/s)
F	Faraday's constant (96000 coulombs/mole)
I	limiting current (Ampere)
J	flux of ferricyanide ($mol/m^2/s$)
L_a	thickness of the agar gel layer (m)
L_i	thickness of medium i (m)
L_f	average biofilm thickness
L_m	thickness of the membrane (m)
L_{ma}	total thickness including the membrane and the agar gel layers (m)
R^2	squared multiple correlation coefficient
S_1	ferricyanide concentration in the upper cell at a given time (mol/m^3)
S_o	initial ferricyanide concentration in the lower cell (mol/m^3)
t	time (s)
v	velocity of liquid in the bulk liquid (m/s)
V_1	volume of upper cell (m^3)
V_2	volume of lower cell (m^3)
X_a	agar gel density (kg/m^3)
z	distance from the bottom of the biofilm (m)

Greek symbol

δ	mass transfer boundary layer thickness near microelectrode tip (m)

Subscripts

a	agar gel
i	subscript shows medium (a, m, ma)
k	number of measurement points of local relative effective diffusivity (horizontally)
m	membrane
n	integer 1, 2, … n
ma	membrane + agar gel (total)
p	number of measurement points of surface average relative effective diffusivity (vertically)

*To whom all correspondence should be addressed. Tel.: 1-406-994-5915; fax: 1-406-994-6098; e-mail: zl@erc.montana.edu

INTRODUCTION

It is well known that growth conditions affect biofilm structure (biofilm porosity, distribution of density, distribution of microorganisms), and that the biofilm structure influences the rate and mechanism

of intrabiofilm mass transport. Some researchers have suggested that when flow velocity increases, biofilm density increases, and when substrate concentration increases, biofilms are less dense (Tanyolaç and Beyenal, 1997, 1996; Peyton, 1996; Gantzer *et al.*, 1991; Characklis and Marshall, 1990; Howell and Atkinson, 1976; Atkinson and How, 1974). The goal of this study was to quantify the effects of substrate concentration and flow velocity at which biofilms were grown on effective diffusivity within the biofilms.

Much effort has been devoted to evaluating the effective diffusivity of different substances in biofilms (see review by Stewart, 1998). Mathematical models of homogeneous biofilms require effective diffusivity as an input parameter. Some authors use mathematical models to calculate the effective diffusivity from experimental data (Beyenal *et al.*, 1997; Livingston and Chase, 1989), others assume or borrow the substrate effective diffusivity and use these models to calculate (predict) biofilm activity (Wood and Whitaker, 1998; Elmaleh, 1990; Grady, 1983; Rittmann and McCarty, 1980; Atkinson *et al.*, 1967). Mathematical models of heterogeneous biofilms, such as AQUASIM (Riechert, 1994), require porosity, density, and effective diffusivity as input parameters (Horn and Hempel, 1997; Wanner and Reichert, 1996). Even the most recent generation of biofilm models, which predict biofilm density, porosity, and the shape of the microcolonies, require that the effective diffusivity is known (Picioreanu *et al.*, 1998a,b; Wimpenny and Colasanti, 1997).

Whether the numerical value of effective diffusivity is assumed and then used as an input parameter for biofilm modeling or is measured in a real biofilm, it is expected to be constant for the entire biofilm. However, recent studies have clearly shown that the effective diffusivity in biofilms varies between locations (Beyenal *et al.*, 1998; Fu *et al.*, 1994; Zhang and Bishop, 1994a,b; Zhang *et al.*, 1995), and depends on biofilm structure (De Beer *et al.*, 1997; Bryers and Drummond, 1996; Lawrence *et al.*, 1994). In our laboratory we used microinjections and confocal microscopy to measure effective diffusivity of different substances in biofilms: fluorescein, tetramethyl-rhodamine isothiocyanite-immunoglobulin G (TRITC-IgG), and phycoerythrin, to show how diffusivity depends on biofilm structure (De Beer *et al.*, 1997). Because microinjections are difficult to master and the results of such measurements are difficult to interpret in heterogeneous biofilms, we adapted our technique of measuring local mass transfer coefficient of electroactive species in biofilms (Yang and Lewandowski, 1995) to measure local effective diffusivity. This new technique allows measurements of local variations in effective diffusivity with high spatial resolution (Beyenal *et al.*, 1998).

To measure the local effective diffusivity we use cathodically polarized microelectrodes. In this technique, ferricyanide, $Fe(CN)_6^{-3}$, evenly distributed in the biofilm, is reduced at the tip of the microelectrode to ferrocyanide, $Fe(CN)_6^{-4}$. As a result, a current is generated in the external circuit, according to the reaction: $Fe(CN)_6^{-3} + e^- \rightarrow Fe(CN)_6^{-4}$. Increasing the polarization potential applied to the microelectrode causes the current to increase until the concentration of $Fe(CN)_6^{3-}$ at the electrode surface reaches zero ($C_s = 0$). The current corresponding to a zero surface concentration of the reacting species is called 'the limiting current'. The flux of ferricyanide, J, to the surface of the microelectrode with sensing area A is related to the limiting current, I, and is given by the equation:

$$J = \frac{I}{bAF} \tag{1}$$

where F is Faraday's constant and b is the number of moles of electrons transferred in the reaction. From the first Fick's law the flux is also related to diffusivity of ferricyanide (D_{CN}) at limiting current condition ($C_s = 0$):

$$J = D_{CN}\frac{C_o - C_s}{\delta} = D_{CN}\frac{C_o}{\delta} \tag{2}$$

Combining eqns 1 and 2 shows that the limiting current generated in the polarization circuit depends on diffusivity of electroactive species in the surrounding medium and, therefore, reflects the rate of mass transport to the tip of the microelectrode. We related the local limiting current density (I/A) to the local effective diffusivity near the microelectrode tip by calibrating the microelectrodes in layers of agar gels of different densities, and of known effective diffusivities for the ferricyanide. All results of diffusivity measurements were normalized by dividing the effective diffusivity of ferricyanide by molecular diffusivity of ferricyanide in the electrolyte solution; results were reported as relative effective diffusivities in the biofilm.

Figure 1 shows the different types of relative effective diffusivity measurements we used in this work. In our previous papers we demonstrated that local effective diffusivities (Beyenal *et al.*, 1998) and local mass transfer coefficients (Yang and Lewandowski, 1995) varied between locations in biofilms. Individual measurements of local relative effective diffusivity, D_l, do not reveal the structured patterns of diffusivity distribution found in biofilms (Fig, 1A). To expose these patterns, local measurements were averaged in a way that demonstrated spatial distribution of effective diffusivity at predetermined distances from the bottom. We measured the D_l at a grid of locations equidistant from the bottom and averaged them as shown in Fig. 1B. The average of these individual D_l measurements at equal distances from the bottom is termed surface averaged relative effective diffusivity (D_s) for the specific distance from the bottom. The average of

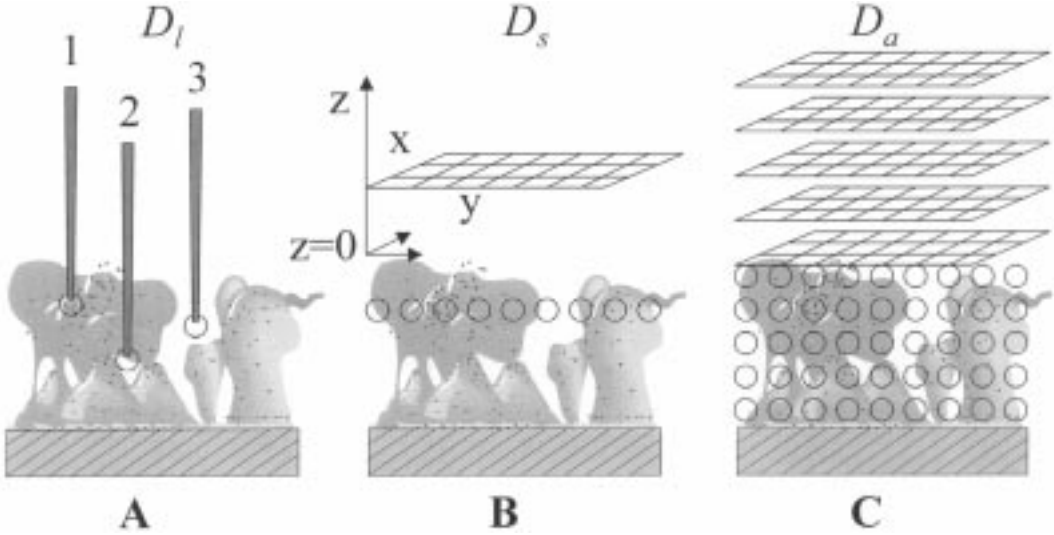

Fig. 1. The system of diffusivity measurements we used in this work. (A) Local relative effective diffusivity (D_l) measured by microelectrodes at arbitrarily selected locations, at different distances from the bottom; (B) The D_l are measured at grid points equally distant from the bottom. The measured D_l are then averaged which gives the surface averaged relative effective diffusivity,

$$D_s = \sum_{n=1}^{k} D_{ln} /k;$$

(C) The average relative effective diffusivity,

$$D_a = \sum_{n=1}^{p} D_{sn}/p,$$

is average of all local measurements for the entire biofilm.

all the D_l measurements at different distances from the bottom is termed average relative effective diffusivity (D_a) and represents the diffusivity for the entire biofilm (Fig. 1C). Using such a system, we quantified the effects of growth conditions, glucose concentration and flow velocity, on the relative effective diffusivities in heterogeneous biofilms.

MATERIALS AND METHODS

Reactor and biofilms

An open channel flow reactor made of polycarbonate, 3.5 cm deep, 2.5 cm wide, and 85 cm long with a total working volume of 400 ml was sterilized using 70% alcohol before each experiment. The nutrient solution was made of KH_2PO_4 (0.35 g/l), Na_2HPO_4 (1.825 g/l), $(NH_4)_2SO_4$ (0.1 g/l), $MgSO_4 \times 7H_2O$ (0.01 g/l), yeast extract (0.01 g/l) and glucose (different concentration for each experiment). To inoculate the reactor, we used one mL portions of *Pseudomonas aeruginosa, Pseudomonas fluorescens*, and *Klebsiella pneumonia*, environmental isolates from the stock at the Center for Biofilm Engineering. The reactor was first operated batch-wise for 12 h and then in continuous flow mode for 5 days. The biofilms were grown at room temperature, $25 \pm 2^{\circ}C$, using combinations of different average flow velocities (3.2, 10, and 25 cm/s) and glucose concentrations (50, 100, 150, 200, 250, and 300 mg/l). Peristaltic pumps (Cole–Parmer, Chicago, IL) were used to maintain flow and to recycle the nutrients. The recycle ratio was greater than 30 for the lowest flow velocity and was increased accordingly for higher flow velocities. The hydraulic retention time was less than 10 minutes to prevent growth of microorganisms in suspension and to keep the substrate concentration constant in the reactor. Glucose concentration in the reactor was measured using procedure 510 by Sigma® Diagnostics. The difference between the influent and effluent glucose concentrations was consistently less than 10% of that in the influent. The recycled solution was continuously aerated in a mixing chamber before entering the reactor. Dissolved oxygen concentration was monitored using a dissolved oxygen electrode.

Effective diffusivity of ferricyanide in agar gel layers

To measure effective diffusivity of ferricyanide in agar gels layers, we used a diffusion cell consisting of two well mixed polycarbonate tanks, each 11 cm deep, 10 cm wide, and 10 cm long, positioned one above another, and separated by a dialysis membrane (Spectrum®, 132709, La Cadena, CA). A fresh membrane was used for each experiment. A suspension of agar (BBL 11853—Becton Dickinson Microbiology Systems, Cockeysville, MD) in 0.2 M KCl was heated to 100°C (in boiling water), then cooled to 40–60°C and carefully poured onto the dialysis membrane. The lower tank (1.040 l working volume) was filled with 0.025 M $K_3Fe(CN)_6$ in 0.2 M KCl, while the upper tank (0.560 l working volume) was filled with 0.2 M KCl. The ferricyanide diffused from the lower tank through the membrane and the agar gel layer into the upper tank. The entire diffusion cell was immersed in a water bath and operated at $25 \pm 1^{\circ}C$. As time progressed, the ferricyanide diffused to the upper tank and its concentration was measured spectrophotometrically at a wavelength of 430 nm. The total mass of ferricyanide in the system estimated at the beginning and at the end of each experiment remained the same within experimental error,

which demonstrated that the accumulation of ferricyanide in the membrane and in the agar gel was negligible. The accumulated volume of liquid collected from the upper tank used to measure ferricyanide concentration amounted to 6 ml and was insignificant compared to the volume of the tank (560 ml). Our assumption that the volume of the ferricyanide solution did not change during measurements simplified calculations.

The mass transfer rate to the upper tank was equivalent to the accumulation rate of ferricyanide in the upper tank. It was quantified for (1) the membrane alone (i = m) and (2) the membrane and agar gel together (i = ma), using eqn (3).

$$D_i \frac{S_o - S_1(1 + V_1/V_2)}{L_i} A_d = V_1 \frac{dS_1}{dt} \tag{3}$$

To find experimental conditions that would justify neglecting external mass transfer limitations in eqn (3), we ran several measurements at increasing agitation rates. We selected an agitation rate of 200 rpm and tested that the mass transport rate did not increase for higher agitation rates. Following the procedure described by Converti *et al.* (1995), eqn (3) was solved for initial conditions, $t = 0$ and $S_1 = 0$, which yielded the effective diffusivity:

$$D_i = \frac{V_1 V_2 L_i}{A_d (V_1 + V_2)(t_n - t_{n-1})}$$

$$\ln\left(\frac{S_o - [(V_1 + V_2)/V_2]S_{1,n-1}}{S_o - [(V_1 + V_2)/V_2]S_{1,n}}\right) \tag{4}$$

From eqn (4), using a series of measured ferricyanide concentrations at different times, we calculated the total effective diffusivity, through the membrane and the agar, D_{ma}, and through the membrane alone, D_m. From these results we calculated the effective diffusivity through the agar gel only, D_{ag}, using eqn (5) (Converti *et al.*, 1995):

$$D_{ag} = \frac{L_a D_{ma} D_m}{L_{ma} D_m - L_m D_{ma}} \tag{5}$$

Within the range of applied agar densities (from 2.5 to 100 g/l), the effective diffusivity of ferricyanide decreased with increasing agar density, and following a curve that was closely fit by the quadratic eqn (6) ($R^2 = 0.99$).

$$D_{ag} = 3.72 \times 10^{-10} - 5.43 \times 10^{-12} X_a + 2.79 \times 10^{-14} X_a^2 \tag{6}$$

Limiting current density (I/A)

Limiting current density was measured using microelectrodes with tip diameters around 10 μm. The construction of the microelectrodes is described elsewhere (Yang and Lewandowski, 1995). We used a commercial calomel electrode (Model 13-620-51, Fisher Scientific, Pittsburgh, PA) as the counter/reference electrode. A Hewlett Packard 4140B Multimeter served as a voltage source and a picoammeter. Molar concentration of ferricyanide in the solution exceeded that of oxygen by two orders of magnitude; we found that oxygen presence in the solution did not influence the results. We used a polarization potential of -0.8 V in all measurements. All measurements were conducted under stagnant conditions, without flow, to eliminate convection.

Local effective diffusivity

Because the limiting current measured by the microelectrodes depended on the local effective diffusivity, the microelectrodes had to be calibrated. We used agar gels of known densities (from 2.5 to 100 g/l) and, consequently, of known effective diffusivities (from the diffusion cell measurements).

The appropriate amount of agar to reach the desired density was added to a solution of 0.025 M $K_3Fe(CN)_6$ and 0.2 M KCl, and was slowly heated until the agar dissolved, then slowly cooled to 40–60°C, and finally poured as layers 250–1000 μm thick on the bottom of the flat plate reactor (without biofilm). After the agar layer solidified, the reactor was carefully filled with a solution of 0.025 M $K_3Fe(CN)_6$ in 0.2 M KCl. The solution was recirculated for two hours to equilibrate the ferricyanide with the agar. During the microelectrode measurements, the flow was stopped and the electrolyte solution remained stagnant. The microelectrodes were mounted on a micromanipulator (Model M3301L, World Precision Instruments, New Haven, CT) equipped with a stepper motor (Model 18503, Oriel, Stratford, CT) controlled by the Oriel Model 20010 interface. Microelectrodes were introduced from the top of the reactor, perpendicularly to the agar gel layer. The measured limiting current density remained constant within the top layers of agar gel but decreased suddenly just above the bottom of the reactor (Fig. 2). We believe that this effect was produced by mass transfer limitations to the microelectrode near the bottom. This effect, also noticed by Beyenal *et al.* (1998) and Yang and Lewandowski (1995), invalidated application of the microelectrodes at distances less than 60 μm from the bottom. Consequently, the results of the limiting current measurements for distances less than 60 μm from the bottom were ignored.

The relation between the limiting current density measured by the microelectrodes and the effective diffusivity of ferricyanide in the agar gel layers was linear within the range of tested agar densities (2.5 to 100 g/l, Fig. 3, $R^2 = 0.97$):

$$D_{ag} = 1.12 \times 10^{-10} + 3.69 \times 10^{-12} (I/A) \tag{7}$$

Local effective diffusivity distribution in biofilms

Before measuring local effective diffusivities in biofilms, we replaced the nutrient solution in the biofilm reactor with the electrolyte. We gently flushed the system with 0.2 M KCl to remove the nutrient solution. Then we replaced 0.2 M KCl with a solution of 0.025 M $K_3Fe(CN)_6$ in 0.2 M KCl. This procedure did not seem to affect the biofilm structure (Yang and Lewandowski, 1995). The ferricyanide solution was recycled for two hours. The temperature during measurements was 25 ± 2°C. Ferricyanide and dissolved oxygen were not consumed by the biofilm under these conditions (results not shown). We measured dissolved oxygen concentration profiles using Clark type microelectrodes with a guard cathode, as described by Revsbech, (1989). The concentration of ferricyanide was measured using similar microelectrodes to those used to measure local effective diffusivity. The tips of the microelectrodes were covered with 5% cellulose acetate membrane to form a layer of increased mass transport resistance. In this case, the limiting current was proportional to the ferricyanide concentration. The microelectrodes were calibrated in ferricyanide solutions from 0 to 25 mM.

The biofilm reactor was positioned on an X–Y micropositioner stage (Model CTC-462-2 S, Micro Kinetics, Laguna Hills, CA). The microelectrode, attached to a linear micropositioner (Model CTC-322-20, Micro Kinetics), was positioned above the reactor. Both the X–Y and the linear micropositioners were computer controlled through a controller (CTC-283-3, Micro Kinetics) with a positioning precision of 0.1 μm. Custom software was used to simultaneously control the microelectrode movement, the

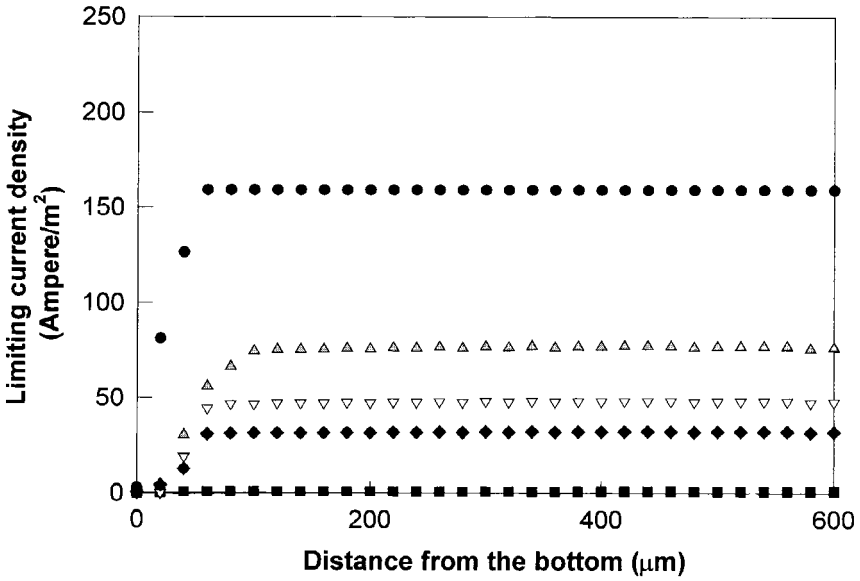

Fig. 2. Variation of local limiting current density with dimensionless distance for different agar densities and effective diffusivities. (● Electrolyte solution; ▲ $D_{ag} = 3.66 \times 10^{-10}$ m^2/s; ▽ $D_{ag} = 3.03 \times 10^{-10}$ m^2/s; ◆ $D_{ag} = 2.24 \times 10^{-10}$ m^2/s; ■ $D_{ag} = 0.99 \times 10^{-10}$ m^2/s).

stage movement, and the data acquisition. At each position of the microelectrode the data acquisition system collected 22 separate readings at a sampling frequency of 1 kHz. The highest and the lowest values were trimmed and the remaining 20 measurements were averaged. The coefficient of variation (CV) was calculated for 20 measurements and the result accepted if the CV was lower than 0.05. When the result was accepted, the microelectrode was moved to the next position. We measured diffusivity at a 10×10 grid matrix with a step size of 100 μm in both X and Y directions. The step size in Z direction was 20 μm. The size of the matrix was selected experimentally. It was expected that biofilm heterogeneity would influence the average diffusivity (that is why we calculated the average; Fig. 1). This effect was expected to be more pronounced if the diffusivity measurements covered a very small area and less pronounced if the size of the area was increased (Gibbs and Bishop, 1995). We repeated the measurements of local effective diffusivity several times at different locations, each time changing the size of the matrix. The average diffusivities from each measurement were calculated and compared. As expected, the differences between these averages were bigger when the matrix was smaller and decreased when the size of the matrix was increased. For practical reasons, we selected a 10×10 matrix, with a step size of 100 μm in each direction. For such conditions the variability between the surface averaged relative effective diffusivity measured at three ran-

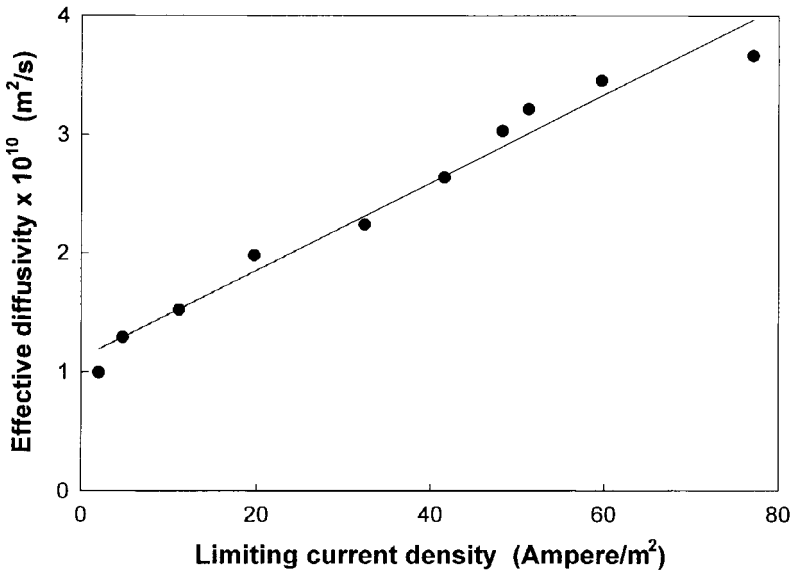

Fig. 3. Calibration curve for the effective diffusivity microelectrode, the effective diffusivity (m^2/s) vs limiting current density (A/m^2) in agar gels of different densities.

domly selected locations was less than 20%. The measurements were conducted 60 cm down stream from the entrance to the reactor, which was more than the entrance length for the highest used flow velocity, calculated according to Bird *et al.*, (1960).

The microelectrode was manually positioned above the first grid point and then moved into the biofilm to a predetermined distance from the bottom using the linear micropositioner. After the limiting current was measured and the data accepted, the linear micropositioner moved the microelectrode out of the biofilm and into the bulk liquid. The motorized X–Y stage moved the reactor to the next grid point, and then the linear micropositioner lowered the microelectrode to the same distance from the bottom as for the previous measurement. Local limiting current densities measured at the same distances from the bottom were used to generate contour maps of local effective diffusivities calculated from eqn 7. Local effective diffusivities measured at the grid points were averaged over the surface for each level in the biofilm to calculate surface averaged effective diffusivities. By dividing the effective diffusivity by the molecular diffusivity of ferricyanide in the electrolyte solution, $D = 7 \times 10^{-10}$ m^2/s, (Gao *et al.*, 1995), we calculated relative effective diffusivity.

RESULTS AND DISCUSSION

Effective diffusivity in agar gels and microelectrode calibration

Limiting current densities measured in agar layers depended on agar concentration (effective diffusivity) and were constant for constant agar density, except for those measured in the close proximity to the bottom. At distances less than 60 μm from the bottom we noticed that the limiting current density was rapidly decreasing (Fig. 2). This effect was reproducible and did not depend on total thickness of the agar layer. It is reasonable to assume that microorganisms growing farther from the bottom experience a spherical pattern of mass transport while those growing closer to the bottom see a different geometrical pattern of mass transport. This argument may be tested if we imagine the pattern of mass transport to a microcolony attached to the bottom of a biofilm reactor: the substrate is delivered only from above and from the sides, the geometry of the mass transport pattern is hemispherical, and the rate of mass transport is about one half of that measured for spherical geometry. The microelectrode measured 'local mass transport rate' which was defined as the mass transport rate to the microelectrode tip. The mass transport rate to the microelectrode tip is inherently inhibited from one side by the presence of the shaft, creating a 'shadow effect' and the other side is inhibited by the presence of the bottom. We believe that these two effects combined caused the observed sudden decrease of the measured limiting current density near the bottom. Since we did not know how to correct our calculations to account for these effects, we disregarded the measurements at distances less than 60 μm from the bottom where the measurements were clearly affected. We also see that this effect limits the applicability of our technique to relatively thick biofilms.

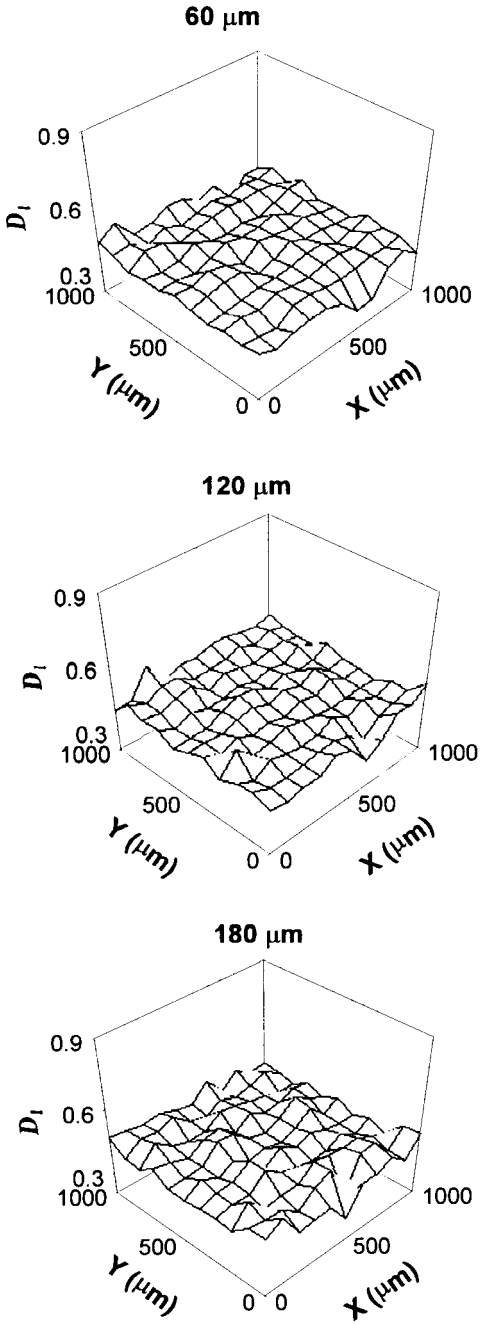

Fig. 4. Horizontal distributions of local relative effective diffusivities (D_l) for biofilms grown at flow velocity 3.2 cm/s and glucose concentration of 50 mg/l at distances 60, 120, and 180 μm from the bottom. The surface averaged relative effective diffusivities were 0.409, 0.426, 0.449 and the standard deviations were 0.0179, 0.0195, and 0.0284, respectively.

For agar gels with densities between 2.5 and 100 g/l, the relation between effective diffusivity and limiting current density was linear (Fig. 3 and eqn 7). For higher agar densities, above 100 g/l, the lim-

iting current density suddenly decreased and the relation between effective diffusivity and limiting current density was nonlinear. It is possible that this effect was caused by technical problems we encountered when penetrating high-density agar with microelectrodes having tip diameters of just a few microns. We assumed, therefore, that microelectrode technique was not suitable for use with agar gels of densities higher than 100 g/l. Fortunately, in our biofilms we did not measure effective diffusivity lower than 0.99×10^{-10} m^2/s, corresponding to agar gels of densities exceeding 100 g/l.

The relation between limiting current density and effective diffusivity of ferricyanide in agar gel eqn (7) is shown in Fig. 3. To test the correctness of the empirical eqn (7), we measured the limiting current density in the electrolyte solution (0.025 M $K_3Fe(CN)_6$ in 0.2 M KCl) and calculated the corresponding diffusivity from eqn (7). The result, 7.02×10^{-10} m^2/s, was very close to the molecular diffusivity of ferricyanide in electrolyte solution, 7×10^{-10} m^2/s (Gao *et al.*, 1995). Additionally, we tested eqn (7) to assure its validity for a different medium (agarose) and the results agreed well with eqn (7) (results not shown).

Horizontal and vertical distribution of relative effective diffusivity

For each biofilm the local relative effective diffusivity (D_l) was measured at several levels. Figure 4 shows an example of such results for a biofilm grown at flow velocity 3.2 cm/s and glucose concentration 50 mg/l at distances 60, 120, and 180 μm from the bottom. The surface averaged relative effective diffusivities were 0.409, 0.426, 0.449 and the standard deviations were 0.0179, 0.0195, and 0.0284, respectively. The D_l varied horizontally and vertically (Fig. 4). For example, at a level 180 μm from the bottom, the highest measured D_l was 0.8 and the lowest was 0.25. We found that the deviations in D_l were associated with the structural elements of our biofilms, such as the presence of interstitial voids separating cell clusters. D_l was up to five times greater in voids than in cell clusters; only small variations in D_l values were observed in cell clusters. To reveal trends in the distribution of D_l at different distances from the bottom we calculated surface averaged relative effective diffusivity (D_s) for each level in the biofilm as presented in Fig. 1.

Horizontal variability of D_l, represented by standard deviations, was used as a measure of structural heterogeneity at each level. Figure 5 shows an example of such analysis using data from Fig. 4. Both the D_s values and the standard deviations (error bars) tend to decrease toward the bottom of the biofilm; we observed similar trends in all biofilms studied. The D_s calculated for all biofilms at different distances from the bottom were normalized for the biofilm thickness. Figure 6 shows the variation of D_s with normalized biofilm depth (z/L_f) for biofilms grown at flow velocities of 3.2 cm/s (a), 10 cm/s (b) and 25 cm/s (c). The measurements in Fig. 6 were taken at 20 μm intervals. To estimate the biofilm thickness at each location, multiply the number of measurements by 20 μm and add 60 μm for the distance from the bottom.

For biofilms grown at flow velocity 3.2 cm/s (Fig. 6a) the D_s decreased with a very low slope toward the bottom of the biofilms. For glucose concentrations of 250 and 300 mg/l, the effective diffusivities were almost equal to the diffusivity in the bulk solution ($D_s \approx 1$). At glucose concentration of 300 mg/l, the D_s near the bottom of the biofilm and

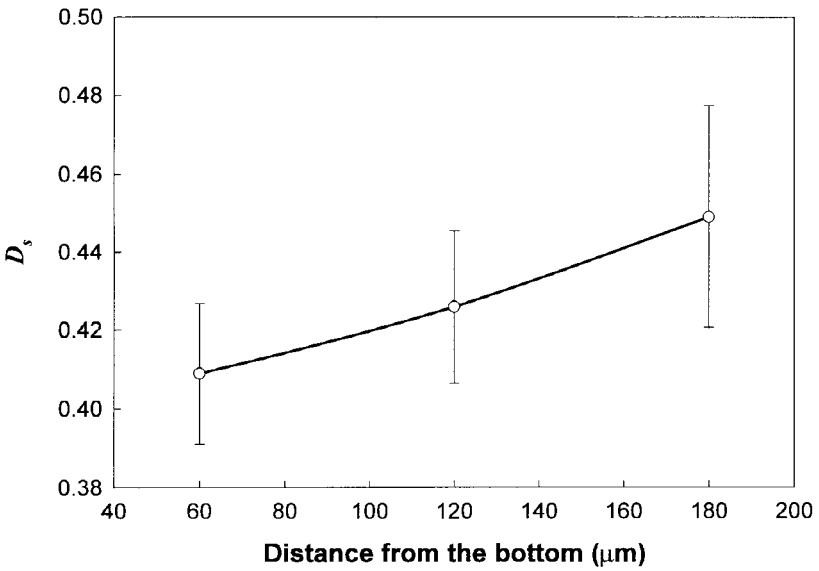

Fig. 5. The D_s vs depth (the data extracted from Fig. 4). The error bars show standard deviations.

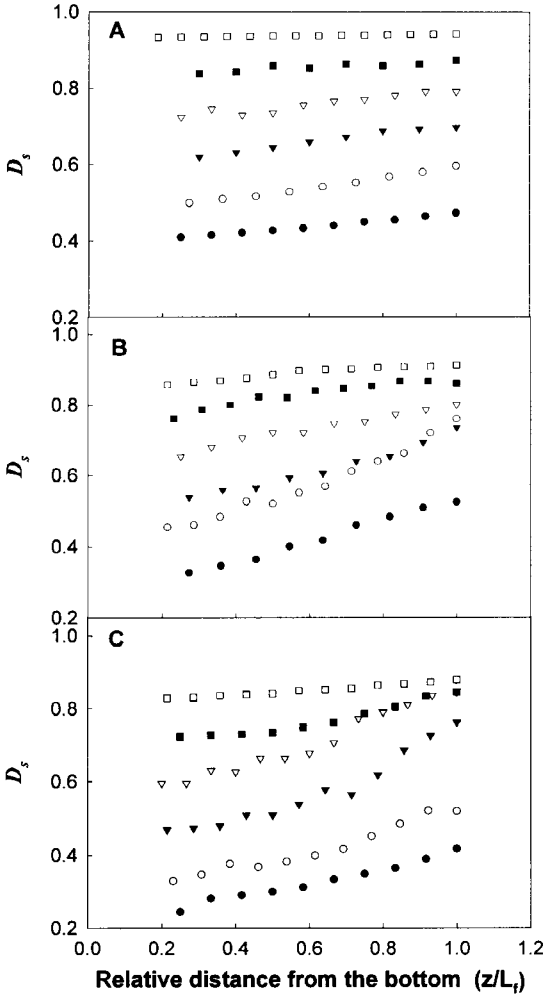

Fig. 6. Variation of D_s with relative distances from the bottom for biofilms grown at flow velocities 3.2 cm/s (A), 10 cm/s (B) and 25 cm/s (C) at different glucose concentrations (● 50 mg/l; ○ 100 mg/l; ▼ 150 mg/l; ▽ 200 mg/l; ■ 250 mg/l; □ 300 mg/l).

at the biofilm surface were 0.94 and 0.96, respectively. At glucose concentration of 50 mg/l, the D_s near the bottom of the biofilm and biofilm surface were 0.40 and 0.46, respectively. These small differences between D_s at the biofilm surface and near the bottom of the biofilm show that the D_s was almost constant with depth for biofilms grown at 3.2 cm/s flow velocity.

For biofilms grown at flow velocity 10 cm/s (Fig. 6b), the D_s decreased towards the bottom. The D_s values for biofilms grown at the same glucose concentrations were lower than those in biofilms grown at 3.2 cm/s flow velocity. Also, the difference between the values of the D_s at the biofilm surface and near the bottom of the biofilm was higher compared to biofilms grown at flow velocity of 3.2 cm/s; the profiles had higher slopes.

For biofilms grown at 25 cm/s flow velocity (Fig. 6c), the D_s decreased towards the bottom. The D_s values for biofilms grown at the same glucose concentration were lower than for biofilms grown at 3.2 and 10 cm/s. For example, for biofilms grown at 50 mg/l glucose concentration and 3.2, 10, and 25 cm/s flow velocities, the D_s near the bottom of the biofilm were 0.4, 0.29 and 0.22, respectively.

At the limit, biofilms grown at 3.2 cm/s and 300 mg/l had D_s values almost equal to diffusivity in the bulk solution ($D_s \approx 1$), for all depths in the biofilm. Consequently, in our biofilms, an assumption of constant (average) effective diffusivity appears to be valid only for biofilms grown at high substrate concentrations and low flow velocities. We found that the D_s for biofilms grown at 300 mg/l glucose concentration was two to three times greater than for biofilms grown at 50 mg/l glucose for each flow velocity. The D_s increased with decreased flow velocity 1.1–1.6 times for the same glucose concentration (Fig. 6a, b and c). We con-

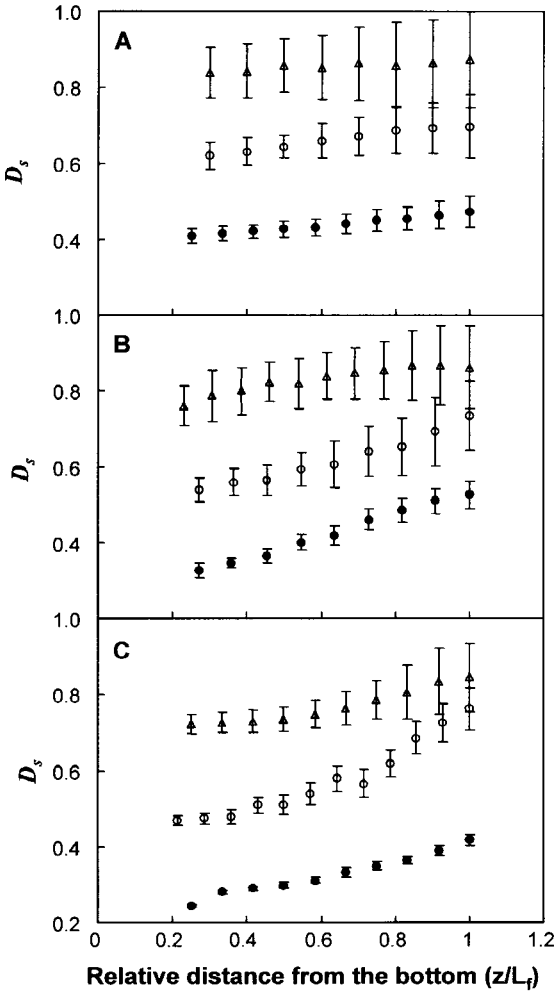

Fig. 7. Variation of D_s and standard deviation from the D_s (error bars) with relative distances from the bottom for biofilms grown at flow velocity of 3.2 cm/s (A), 10 cm/s (B), and 25 cm/s (C), and glucose concentrations of ● 50 mg/l, ○ 150 mg/l and ▲ 250 mg/l.

cluded that the D_s profiles were little affected by the flow velocity but strongly affected by the glucose concentration at which the biofilms were grown.

Zhang *et al.* (1995) measured distributions of effective diffusivity, porosity, and density in biofilms. They found that effective diffusivity and porosity decreased exponentially toward the bottom of the biofilm while density increased. They concluded that biofilm thickness was one of the parameters which controlled the shape of the diffusivity profiles. In our study, biofilm thicknesses were around 250–350 μm. This was a lower variation compared to biofilm thicknesses (80–1170 μm) tested by Zhang *et al.* (1995). Consequently, we may assume that in our biofilms of almost constant thickness, the biofilm thickness did not influence the shape of the diffusivity (D_s) profiles. The only variables were bulk glucose concentration and flow velocity at which biofilms were grown. Figure 6 shows that glucose concentration had a strong influence on the diffusivity (D_s) profiles and the value of the D_s.

The variations of D_s (selected results from Fig. 6) are presented in Fig. 7 along with standard deviations (error bars). The standard deviations were calculated based on the local relative effective diffusivities measured for each specified distance from the bottom. In homogeneous biofilms, standard deviation reflects only the experimental errors. In heterogeneous biofilms standard deviation reflects biofilm heterogeneity. The differences in measured effective diffusivities between locations are caused by the presence of voids and channels in the biofilm matrix. Figure 7 shows selected D_s in biofilms grown at flow velocities 3.2 cm/s (a), 10 cm/s (b) and 25 cm/s (c) and at glucose concentrations of 50, 150, and 250 mg/l. In all cases, the standard deviations were higher when biofilms were grown at higher glucose concentrations and at lower flow velocities. For D_s higher than 0.7, standard deviations were >0.05; for $D_s < 0.7$, the standard deviations were <0.05. If we assume that standard deviations are significant when higher than 0.05 it can be concluded that the standard deviations (and therefore biofilm heterogeneity) are significant when the average relative effective difffusivity is higher than 0.7. Such conditions are associated with biofilms growing at high glucose concentration and at low flow velocities. Also, such conditions are more likely to occur near the biofilm surface than near the bottom.

Multiple linear regression models were constructed for the response variable, D_s, presented in Fig. 6, where the predictor variables were position, glucose concentration and flow velocity at which the biofilms were grown (Kleinbaum *et al.*, 1998). The best-fit model equation is shown in eqn (8). The standard deviation for residuals was 0.03234. Probability values for each coefficient were zero, showing that all variables in eqn (8) affect D_s. Minitab for Windows® version 11.2 (1996) was used to evaluate the best-fit values of coefficients (eqn 8).

$$D_s = 0.25 - 0.95v + 2.3C_g + 0.23(z/L_f) + 0.93vC_g + 0.59v(z/L_f) - 0.7C_g(z/L_f) \quad (8)$$

According to eqn (8), the D_s increases with increasing glucose concentration and position and decreases with increasing flow velocity at which the biofilm was grown. The product terms involving glucose concentration and flow velocity, flow velocity and position, and glucose concentration and position, show their interactive influence on the D_s. The model predictions and experimental obser-

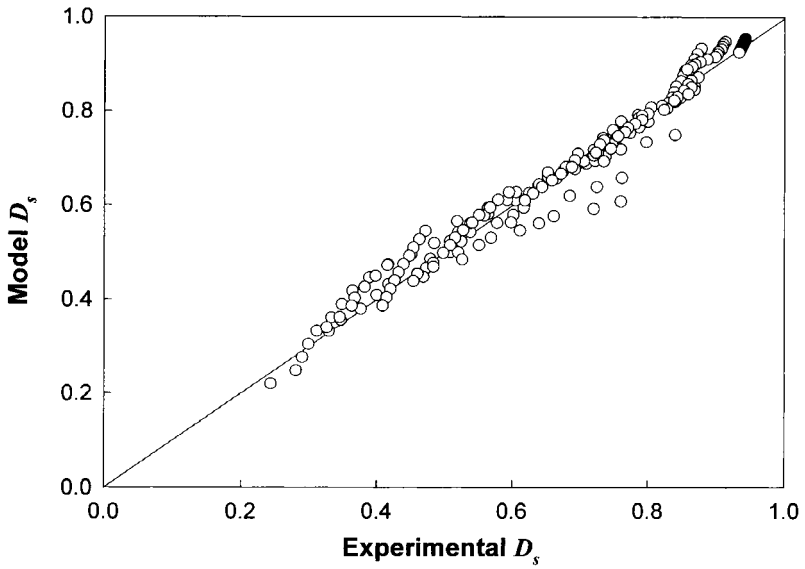

Fig. 8. Model D_s vs experimental D_s ($R^2 = 0.97$).

vations were plotted in Fig. 8 showing good agreement ($R^2 = 0.97$). It is not clear whether effective diffusivity profiles in the biofilms are linear or nonlinear. Fu *et al.* (1994) and Zhang *et al.* (1994a) showed exponentially decreasing effective diffusivity profiles for their biofilms. According to our multiple linear regression model and our experimental observations the diffusivity profiles in the biofilms are generally linear. However, this may be different for different biofilms.

Combined effects of flow velocity and substrate concentration at which the biofilms were grown on average relative effective diffusivity (D_a)

All local measurements of effective diffusivity were combined to calculate the average relative effective diffusivity (D_a) as presented in Fig. 1. The D_a represents an average of relative effective diffusivity for an entire biofilm. Three-dimensional relationships between the D_a, glucose concentration, and flow velocity at which the biofilms were grown are shown in Fig. 9. We found that the D_a varied from 0.9 to 0.3 for biofilms grown at different flow velocities (3.2–25 cm/s) and glucose concentrations (50–300 mg/l). These results correspond well with those already published: relative effective diffusivity of oxygen in *A. niger* pellet from 0.72 to 0.13 (Yano *et al.*, 1961); N_2O relative effective diffusivity in *E. coli* aggregates, from 1 to 0.27 (Libicki *et al.*, 1988); phenol relative effective diffusivity in mixed population biofilms from 0.88 to 0.12 (Livingston and Chase, 1989).

The D_a increased rapidly with increased glucose concentration, and decreased slowly with increased flow velocity at which the biofilm was grown. High D_a at high glucose concentrations indicates lower biofilm density, which is consistent with previously reported observations (Tanyolaç and Beyenal, 1997, 1996; Costerton *et al.*, 1981; Atkinson and How, 1974). For a glucose concentration of 300 mg/l the D_a is only slightly lower than 1, showing that diffusional mass transfer limitations are not significant for these biofilms. Figure 9 shows that the D_a is controlled mainly by the bulk glucose concentration at which the biofilm was grown and reveals that each biofilm had a characteristic D_a depending on growth condition. Our study was conducted on 5 days old biofilms only and it is not clear whether those relations remain unchanged in older biofilms.

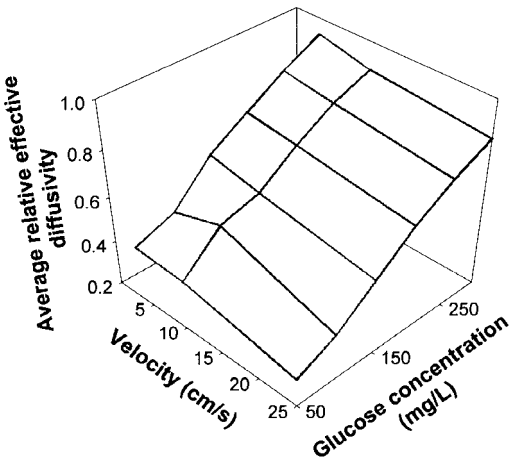

Fig. 9. Average relative effective diffusivities (D_a) vs flow velocities and glucose concentrations at which biofilms were grown.

CONCLUSIONS

For the experimental conditions employed we concluded that in 5 days old, three species biofilms:

1. The D_s in biofilms progressively decreased from top to the bottom.
2. Flow velocity and glucose concentration influenced the D_s profiles.
3. Relative effective diffusivities (both the D_s and the D_a) increased with increase in glucose concentration.
4. Relative effective diffusivities (both the D_s and the D_a) decreased with increase in flow velocity.
5. Glucose concentration had a stronger effect on the relative effective diffusivities (both D_s and D_a) than the flow velocity.

Acknowledgements—The research was supported by the cooperative agreement EED-8907039 between the National Science Foundation and Montana State University. The authors thank Drs Frank Roe and Marty Hamilton from Center for Biofilm Engineering for their valuable comments and discussions.

REFERENCES

Atkinson B., Busch B., Swilley A. W. E. L. and Williams D. A. (1967) Mass transfer and organism growth in a biological film reactor. *Trans. Inst. Chem. Eng.* **45**, 257–264.

Atkinson B. and How S. Y. (1974) The overall rate of substrate uptake (reactor) by microbial film-2. Effect of concentration and thickness with mixed biological films. *Trans. Inst. Chem. Eng.* **52**, 260–268.

Beyenal H., Şeker Ş, Salih B. and Tanyolaç A. (1997) Diffusion coefficients of phenol and oxygen in a biofilm of *Pseudomonas putida*. *AIChE J* **43**, 243–250.

Beyenal H., Tanyolaç A. and Lewandowski Z. (1998) Measurement of local effective diffusivity in heterogeneous biofilms. *Wat. Sci. Tech.* **38**, 171–178.

Bird R. B., Steward W. E. and Lightfoot E. N. (1960) *Transport Phenomena*. John Wiley & Sons, Singapore.

Bryers D. J. and Drummond F. (1996) Local mass transfer coefficients in bacterial biofilms using fluorescence recovery after photobleaching (FRAP). In *Progress in Biotechnology 11, Immobilized Cell: Basics and Applications*, eds R. H. Wijffels, R. M. Buitelaar, C. Bucke and J. Tramper, pp. 196–204. Elsevier, New York.

Characklis W. G. and Marshall K. C. (1990) *Biofilms*. Wiley, New York, pp. 397–443.

Converti A., Casagrande M., De Giovanni M., Rovatti M. and Del Borghi M. (1995) Evaluation of glucose dif-

fusion coefficient through cell layers for the kinetic of an immobilized cell bioreactor. *Chem. Engng. Sci.* **51**, 1023–2026.

Costerton J. W., Irvin R. T. and Cheng K. J. (1981) The bacterial glycocalyx in nature and disease. *Annu. Rev. in Microbiology* **35**, 299–324.

De Beer D., Stoodley P. and Lewandowski Z. (1997) Measurement of local diffusion coefficients in biofilms by microinjection and confocal microscopy. *Biotechnol. Bioeng.* **53**, 151–158.

Elmaleh S. (1990) Rule of thumb modeling of biofilm reactors. *Wat. Sci. Tech.* **22**, 405–418.

Fu Y-C., Zhang T. C. and Bishop P. L. (1994) Determination of effective oxygen diffusivity in biofilms grown in a completely mixed biodrum reactor. *Wat. Sci. Tech.* **29**, 455–462.

Gantzer C. J., Rittmann B. E. and Herricks E. E. (1991) Effects of long term water velocity changes on streambed biofilm activity. *Wat. Res.* **25**, 15–20.

Gao X., Lee J. and White H. S. (1995) Natural convection at microelectrodes. *Anal. Chem.* **67**, 1541–1545.

Grady Jr C. P. (1983) Modeling of biological fixed films—A state of the art review. In *Fixed Film Biological Process for Wastewater Treatment*, eds Y. C. Wu and E. D. Smith, pp. 75–134. Noyes Data Corporation, New Jersey.

Gibbs J. T. and Bishop P. L. (1995) A method for describing biofilm surface roughness using geostatistical techniques. *Wat. Sci. Tech.* **32**, 91–98.

Horn H. and Hempel D. C. (1997) Substrate utilization and mass transfer in an autotrophic biofilm system: Experimental results and simulation. *Biotechnol. Bioeng.* **53**, 363–371.

Howell J. A. and Atkinson B. (1976) Sloughing of microbial film in trickling filters. *Wat. Res.* **10**, 307–315.

Kleinbaum D. G., Lawrance L. K. and Muller K. E. (1998) *Confounding and Interaction in Regression Analysis and Other Multivariable Methods.* Pws-kent publishing company, Boston, pp. 163–174.

Lawrence J. R., Wolfaardt G. M. and Korber D. R. (1994) Determination of diffusion coefficients in biofilms by confocal laser microscopy. *Applied and Environmental Microbiology* **60**, 1166–1173.

Libicki S. B., Salmon P. M. and Robertson C. R. (1988) The effective diffusive permeability of a nonreacting solute in microbial cell aggregates. *Biotechnol. Bioeng.* **32**, 68–85.

Livingston A. G. and Chase H. (1989) Modeling of phenol biodegradation in a fluidized-bed bioreactor. *AIChE J* **35**, 1980–1992.

Peyton B. M. (1996) Effects of shear stress and substrate loading rate on *Pseudomonas aeruginosa* biofilm thickness and density. *Wat. Res.* **30**, 29–36.

Picioreanu C., van Loosdrecht M. C. M. and Heijnen J. J. (1998a) A new combined differential-discrete cellular automaton approach for biofilm modeling: Application for growth in gel beads. *Biotechnol. Bioeng.* **57**, 718–731.

Picioreanu C., van Loosdrecht M. C. M. and Heijnen J. J. (1998b) Mathematical modeling of biofilms structure with a hybrid differential—discrete cellular automaton approach. *Biotechnol. Bioeng.* **58**, 101–116.

Revsbech N. P. (1989) An oxygen microsensor with a guard cathode. *Limnol. Oceanogr.* **34**, 474–478.

Riechert P. (1994) AQUASIM—a tool for simulation and data analysis of aquatic systems. *Water Sci. Tech.* **30**, 21–30.

Rittmann B. E. and McCarty P. L. (1980) Model of steady-state biofilm kinetics. *Biotechnol. Bioeng.* **22**, 2343–2357.

Stewart P. (1998) A review of experimental measurements of effective diffusive permeabilities and effective diffusion coefficients in biofilms. *Biotechnol. Bioeng.* **59**, 261–272.

Tanyolaç A. and Beyenal H. (1996) Predicting average biofilm density of a fully active spherical bioparticle. *Journal of Biotechnology* **52**, 39–49.

Tanyolaç A. and Beyenal H. (1997) Prediction of average biofilm density and performance of a spherical particle under substrate inhibition. *Biotechnol. Bioeng.* **56**, 319–329.

Wanner O. and Reichert P. (1996) Mathematical modeling of mixed culture biofilms. *Biotechnol. Bioeng.* **49**, 172–184.

Wimpenny J. W. and Colasanti R. (1997) A unifying hypothesis for the structure of microbial biofilms based on cellular automanton models. *FEMS Microbiology Ecology* **22**, 1–16.

Wood B. D. and Whitaker S. (1998) Diffusion and reaction in biofilms. *Chem. Eng. Sci.* **53**, 397–425.

Yang S. and Lewandowski Z. (1995) Measurement of local mass transfer coefficient in biofilms. *Biotechnol. Bioeng.* **48**, 737–744.

Yano T., Kodama T. and Yamada K. (1961) Fundemantel studies on the aerobic fermentation. Part VII. Oxygen transfer within a mold pellet. *Agr. Biol. Chem.* **25**, 580–584.

Zhang T. C. and Bishop P. L. (1994a) Evaluation of tortuosity factors and effective diffusivities in biofilms. *Wat. Res.* **28**, 2279–2287.

Zhang T. C. and Bishop P. L. (1994b) Density, porosity, and pore structure of biofilms. *Wat. Res.* **28**, 2267–2277.

Zhang T. C., Fu Y. C., Bishop P. L., Kupferle M., FitzGerald S., Jiang H. H. and Harmer C. (1995) Transport and biodegradation of toxic organics in biofilms. *J. Hazardous Materials* **41**, 267–285.